Impact of Directional Antenna of Primary System Receiver in Spectrum Sensing: A Case Study

Yoshimitsu Yagi, Takuto Ohno, Hidekazu Murata, *Member, IEEE,* Koji Yamamoto, *Member, IEEE,* and Susumu Yoshida, *Member, IEEE,*

***Abstract*—In cognitive radios, a directional antenna can be used at the primary system receiver in order to improve reception performance. The problem is that the cognitive radio sensors may not detect weak signals from the primary system transmitter far away, whereas these signals can be received by a high-sensitivity primary system receiver. The present paper describes the experimental results obtained in field trials performed in order to demonstrate the impact of various parameters (e.g., directional gain, reflections, and diffractions) in spectrum sensing.**

***Index Terms*—cognitive radio, experimental study, spectrum sensing, directional antenna.**

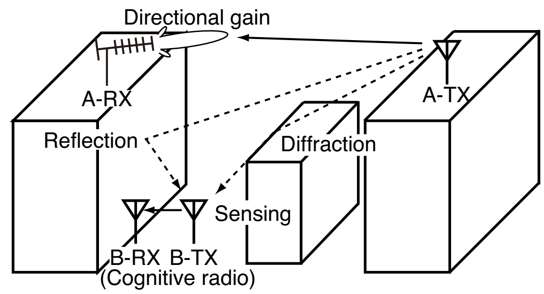

Fig. 1. System scenario. Group A is a high-priority system, and group B is a cognitive radio system (low-priority system). A-RX uses a directional antenna. We must take into account the 3D pattern for the directional antenna, reflections, and diffractions outside the building.

I. Introduction

In cognitive radio systems [1], [2], a directional antenna can be used at the primary system receiver to receive weak signal from the transmitter far away. The directional antenna provides the advantages of higher gain because, unlike the omnidirectional antenna, the directional antenna can focus energy in one particular direction. Furthermore, the directional antenna at the fixed primary system receiver is generally mounted on the roof of the building in order to establish LOS.

On the other hand, the mobile cognitive radio often uses an omnidirectional antenna. The antenna height is much lower than the building height because the cognitive radio is a mobile station. In order to overcome these disadvantages, the cognitive radio must have better sensitivity than the primary system. However, it is unrealistic to drastically reduce the noise figure or take the long averaging time. The problem arises when the cognitive radio must robustly detect a weak signal from the primary system transmitter. The cognitive radio may not detect weak signals from the transmitter in the primary system, whereas these signals can be received by the high-sensitivity receiver in the primary system (e.g., using the directional antenna). As a result, the cognitive radio may not protect the communication of the primary system.

The required sensitivity for the cognitive radio is dependent on the sensitivity of the primary system and the relative positions of the cognitive radio and primary system. Therefore, we must take into account 3D patterns for the directional antenna, reflections, and diffractions outside the building. The present paper describes experimental results obtained through field trials conducted as a case study. Through this case study, we demonstrate the impact of various parameters (e.g., directional gain, reflections, and diffractions) in spectrum sensing.

Y. Yagi, T. Ohno. H. Murata, K. Yamamoto, and S. Yoshida are with the Graduate School of Informatics, Kyoto University, Kyoto, Japan (e-mail: contact-h22@hanase.kuee.kyoto-u.ac.jp).

Manuscript received August 12, 2010; revised August 12, 2010.

II. System scenario

As shown in Fig. 1, two source-destination pairs, group A and group B, share the same frequency band. The stations in group A are high-priority (primary) users, whereas the stations in group B are cognitive radios, which are considered to be low-priority (secondary) users. A-RX uses a directional antenna and receives a weak signal from A-TX. Group A does not provide any information for spectrum sharing (e.g., the signal level from B-TX received at A-RX) to group B. Moreover, group B has no position information pertaining to group A.

In order to avoid interference with A-RX, B-TX does not start transmission to B-RX when the presence of A-TX is detected. For simplicity, we use the energy detection method described in [3], [4] instead of cyclostationary feature detection [5]. In this experiment, we ensure that only B-TX detects the presence of A-TX. Here, the decision of the presence of A-TX is defined by D and is given by

$$D = \begin{cases} 0 & P_{\mathrm{A,B\text{-}TX}} < T_{\mathrm{detect}}, \\ 1 & P_{\mathrm{A,B\text{-}TX}} \geq T_{\mathrm{detect}}, \end{cases} \tag{1}$$

where $P_{\mathrm{A,B\text{-}TX}}$ is the signal level received by B-TX from A-TX, and T_{detect} is the signal sense threshold. In other words, if $P_{\mathrm{A,B\text{-}TX}}$ does not exceed the signal detection threshold T_{detect}, B-TX starts transmission to B-RX.

III. Hardware architecture

Fig. 2 shows the hardware architecture of B-TX and B-RX. B-TX is composed of a sensing part and a communication

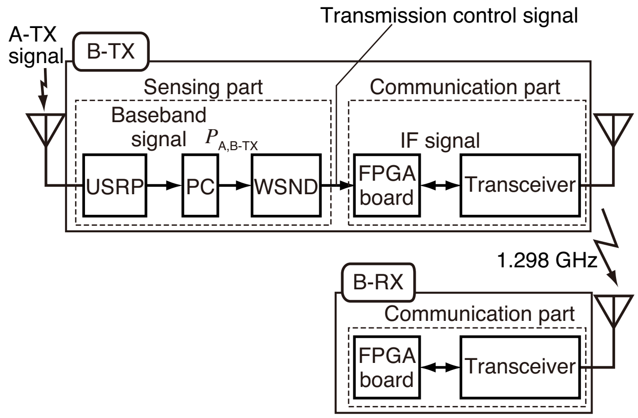

Fig. 2. Hardware architecture of B-TX and B-RX. A-TX and A-RX have the same architecture as B-RX. "WSND" denotes a wireless sensor network device.

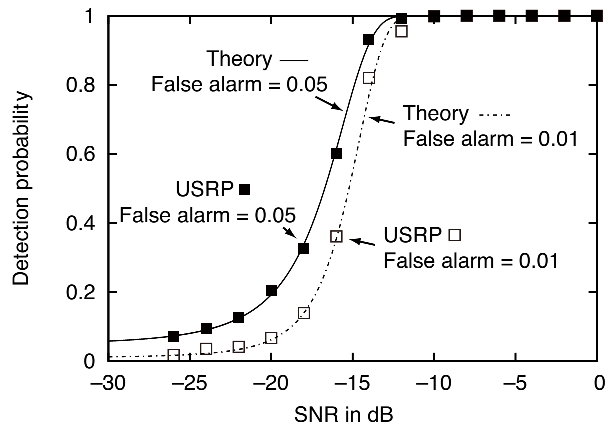

Fig. 3. Detection probability versus SNR.

TABLE I
MAJOR PARAMETERS OF COMMUNICATION PART.

Antenna gain of the directional antenna	17 dBi
Antenna gain of the omnidirectional antenna	2.15 dBi
Carrier frequency	1.298 GHz
TX power of A-TX (directional)	2.0 dBm
TX power of A-TX (omnidirectional)	16.5 dBm
TX power of B-TX (omnidirectional)	8.6 dBm
Antenna height of A-TX	26 m
Antenna height of A-RX	17.5 m
Antenna height of B-TX and B-RX	1.5 m
FPGA	Stratix EP1S25F780C5
Intermediate frequency	10.85 MHz
Modulation	$\pi/4$ shift QPSK
FIR filter	Root roll-off Nyquist (Roll-off factor α = 0.7)
Symbol rate	21.1914 kHz
Packet length	66 symbols
Error detection	CRC-16

part. The communication part includes a transceiver and an FPGA board for data communication over the 1.2-GHz band. The sensing part includes a wireless sensor network device (referred to hereinafter as WSND), a universal software radio peripheral (USRP) [6], and a personal computer (PC) for sensing A-TX. The stations in group A have only the communication part, similar to B-RX.

A. Sensing part

1) WSND: This device is equipped with a 2.4-GHz IEEE 802.15.4 radio chip, general-purpose I/O pins, a battery, a CPU, and other components. In addition, this device can be programmed using Java. In this experiment, the WSND is used to determine whether signal transmission should be carried out. If $P_{\mathrm{A,B\text{-}TX}}$ does not exceed T_{detect}, the WSND of B-TX outputs the signal via a general-purpose I/O pin in order to allow transmission from the communication part.

2) USRP: The USRP system consists of a motherboard and changeable plug-in daughterboards. The motherboard and daughterboard perform interpolation/decimation, up/downconversion, signal amplification, and conversion to/from the analog and digital signal domains. The host PC receives I and Q signals through the USB. The USRP complements the GNU Radio software for the development of software radios. GNU Radio is an open-source software toolkit that provides a library of signal processing blocks for developing communication systems.

In this experiment, the USRP is used as an energy detector. In this method, the processing gain is proportional to the FFT size N and the number of observation/averaging T [3]. In this experiment, we set $N = 512$ and $T = 39$, and the A/D sampling frequency is 500 kHz. M bins are averaged over T times, and here, $M = 66$. As a result, the frequency resolution is 0.98 kHz. Fig. 3 shows that the detection probability curve obtained from the USRP is approximately consistent with the theoretical curve obtained from [7].

B. Communication part

Circuits that generate the baseband and the IF signals are implemented in the FPGA board. In A-TX and B-TX, the transceiver upconverts the IF signal generated by the FPGA board to the RF signal. In A-RX and B-RX, on the other hand, the transceiver downconverts the RF signal to the IF signal before demodulation by the FPGA board.

IV. EXPERIMENTAL SETUP AND RESULTS

The major parameters of the communication part are shown in Table I. In this experiment, the WSND repeats the same process. First, the WSND receives $P_{\mathrm{A,B\text{-}TX}}$ from the PC through the USB. Here, $P_{\mathrm{A,B\text{-}TX}}$ is averaged over the last 39 cycles by the PC. On the basis of the averaged $P_{\mathrm{A,B\text{-}TX}}$, the WSND determines whether to transmit. An example of the sensing operation at B-TX is shown in Fig. 4.

The trial layout is shown in Fig. 5. In this experiment, the detection performance is evaluated at two positions, P1 and P2. A-RX uses a directional antenna (17-element loop Yagi antenna) and receives the weak signal from A-TX. Here, the transmission power of A-TX is 2.0 dBm. A 20-dB attenuator is inserted into A-RX in order to eliminate the influence of the leakage power from A-TX, the shielding of which is not completely effective. For comparison, an omnidirectional antenna (half-wave whip antenna) is also employed in A-RX, and the transmission power of A-TX is set to 16.5 dBm. In both situations, the power levels received at A-RX, i.e., -89 dBm, are the same.

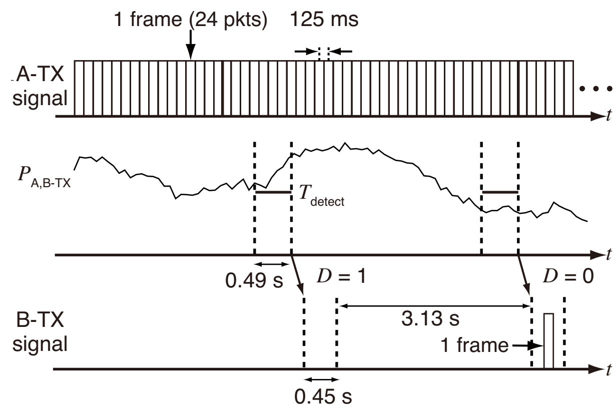

Fig. 4. Time structure of the experimental system.

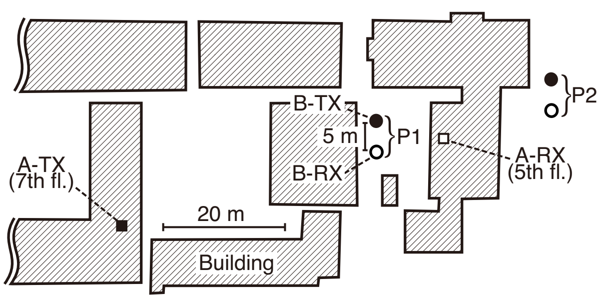

Fig. 5. Location of stations in the trial area.

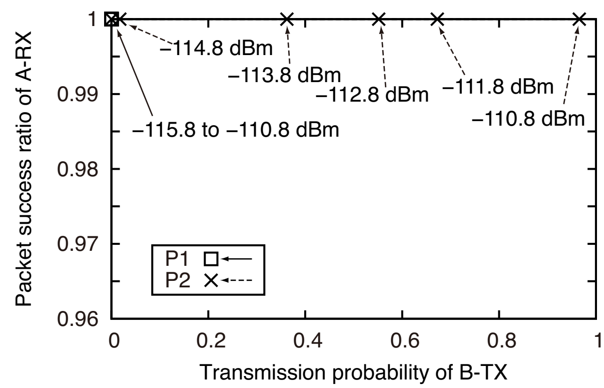

Fig. 6. Packet success ratio of A-RX using the omnidirectional antenna vs. transmission possibility of B-TX. Various detection thresholds are considered. The transmission power of A-TX is set to 16.5 dBm in order to assume the scenario in which B-TX senses a strong signal from the nearby A-TX.

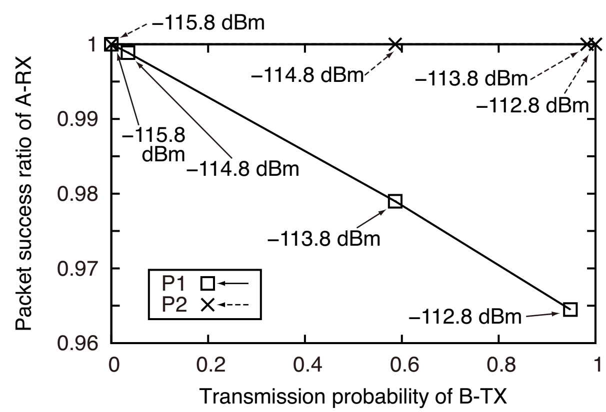

Fig. 7. Packet success ratio of A-RX using a directional antenna vs. transmission possibility of B-TX. Various detection thresholds are considered. The transmission power of A-TX is set to 2.0 dBm in order to assume the scenario in which B-TX senses a weak signal from A-TX far away.

Figs. 6 and 7 show the plot of the packet success ratio of A-RX versus the transmission possibility of B-TX at P1 and P2. In each configuration, these values are obtained during a 3-min observation time. In this experiment, the number of received packets at B-RX is exactly equal to the number of transmitted packets at B-TX because there is no interference with B-RX from A-TX. T_{detect} is changed in 1-dB steps in order to compare the detection performance at different thresholds.

As shown in Fig. 6, an optimum threshold exists for the cognitive radio. When $T_{\text{detect}} = -110.8$ dBm, B-TX at P2 can transmit all packets while avoiding interference with A-RX, and B-TX at P1 can avoid interference with A-RX. Thus, if B-TX uses this threshold, it can opportunistically access the spectrum without causing interference with the high-priority A-RX.

On the other hand, as shown in Fig. 7, it is difficult for the cognitive radio to identify the optimum threshold for opportunistic secondary access without causing any interference with the high-sensitivity primary system. When $T_{\text{detect}} = -113.8$ dBm, B-TX at P2 can transmit all packets without any interference with A-RX. However, B-TX at P1 causes harmful interference with A-RX. Moreover, when $T_{\text{detect}} = -115.8$ dBm, B-TX at P1 may not cause any interference with A-TX, whereas B-TX at P2 largely prevents transmission. Thus, this lower detection threshold decreases the miss detection probability, while increasing the possibility of a false alarm under noise uncertainty.

V. Conclusion

We have clarified the impact of the directional patterns of a primary system receiver in cognitive radio systems through an experimental case study. It is confirmed that the directional antenna of the primary system receiver may introduce additional tradeoff in selecting the threshold.

References

[1] J. Mitola III and G. Q. Maguire Jr. , "Cognitive radio: Making software radios more personal," *IEEE Personal Commun.*, vol. 6, no. 4, pp. 13–18, Aug. 1999.
[2] S. Haykin, "Cognitive radio: Brain-empowered wireless communications," *IEEE J. Sel. Areas Commun.*, vol. 23, no. 2, pp. 201–220, Feb. 2005.
[3] D. Cabric, S. M. Mishra, A. Sahai and R. W. Brodersen, "Implementation issues in spectrum sensing for cognitive radios," *Asilomar Conference on Signals, Systems, and Computers*, vol. 1, pp. 772–776, Nov. 2004.
[4] S. Maharjan, K. Po and J. Takada, "Experimental study of energy detector prototype for cognitive radio system," *IEICE Technical Report, SR2007-52*, vol. 107, no. 352, pp. 43–48, Nov. 2007.
[5] P. J. Green and D. P. Taylor, "A real time cognitive radio test platform for public safety physical layer expriments," *Proc. IEEE PIMRC'07*, pp. 1–5, Sep. 2007.
[6] *http://www.ettus.com/*.
[7] H. Urkowitz, "Energy detection of unknown deterministic signals," *Proc. of the IEEE*, pp. 523–531, Apr. 1967.